35th Annual International Conference of the IEEE EMBS
Osaka, Japan, 3 - 7 July, 2013

Quantitative Analysis of Lymphocytes Morphology and Motion in Intravital Microscopic Images

Yali Huang, Zhiwen Liu, *Member, IEEE*, Yonggang Shi,
Ning Li, Xing An, and Xiaoming Gou, *Student Member, IEEE*

Abstract— **Studying the morphology and interior movement of lymphocytes in intravital microscopic images is essential to understanding and treating various biological processes and pathological situations. A method combing features of shape, deformation, and intracellular motion for quantitatively characterizing the dynamic behavior of a single lymphocyte is proposed in this paper. The method is tested on a set of image sequences of lymphocytes obtained from the peripheral blood of mice undergoing skin transplantation using a phase contrast microscope. Experimental results coincide with the clinical observation and pathological analysis, demonstrating that the extracted cell morphology and motion features can provide new insights into the relationship between the dynamic behavior of lymphocytes and the occurrence of graft rejection.**

I. Introduction

Cell morphology and motility are highly dynamic phenomena that are essential to various biological processes, such as the development of an organism, wound healing, cancer metastasis, inflammation research and immune response [1]. Quantification of cell dynamic behavior through live cell imaging has become a powerful analytical tool for improving our understanding of various biological processes and the relationship between cell activity and pathological situation [2-5]. For example, clinicians have observed that the deformation and motion of lymphocytes are relatively random and occur at high frequencies during the graft rejection process after transplantation. Currently, needle biopsy is the golden standard pathological method to diagnose rejection [6]. However, it is invasive, time-consuming, trial times limited, and dependent on the puncture location. Identification of abnormalities of the dynamic behavior of a single lymphocyte related to graft rejection induced by transplantation might lead to good indictors of the diagnosis of graft rejection. Phase contrast microscopes are one of the most widely used imaging techniques for examining long-term cell behaviors since harmful side effects to living cells are minimized. The lack of quantitative data at the cellular level has hampered theoretical developments of cellular biophysics [7].

*Research supported by National Natural Science Foundation of China (Nos. 61271112 and 60971133).

Yali Huang, Zhiwen Liu, Yonggang Shi, Xing An, and Xiaoming Gou are with School of Information and Electronics, Beijing Institute of Technology, Beijing, China (e-mails: huangyali8888@gmail.com; zwliu@bit.edu.cn; ygshi@bit.edu.cn; anxing512@126.com; xmgou@bit.edu.cn).

Yali Huang is also with College of Electronics and Information Engineering, Hebei University, Baoding, China.

Ning Li is with Department of General Surgery, Beijing You'An Hospital, Beijing, China (e-mail: lining@cbotc.com).

Applications of cell image analysis, such as the classification of white blood cells [8], cell segmentation and tracking [5], the measurement of cell motility and morphology [9], quantitative analysis of cell motion [10, 11], characterization of cell deformation and migration [4], quantitative study of the dynamic behavior of cell [12], and cell shape analysis [3, 13, 14], have been developed in the past decades. In previous work pertaining to the analysis of cell motion, the cell speed was usually calculated via the displacement of the centroid of cell [9], by the tangent direction of the cell motion trail [11], through the cell deformation [13], or via the affine-motion model [4, 12]. All these methods dealt with the whole movement of the cell, while a little attention has been paid to measure intracellular motion [10]. Quantitative methods for cell shape analysis were introduced in [3], however, they didn't provide dynamic information about cell activity. The work described in [10, 11] only dealt with cell motion analysis. There are few approaches that combined the two aspects of cell morphology and motion[9]. Our group has presented a geometric method for modeling dynamic features of cells in image sequences, which emphasized cell deformation analysis without considering intracellular movement [15].

In this paper, we quantitatively analyze the dynamic behavior of a single lymphocyte from three aspects: shape, deformation and intracellular motion. The three features are combined to characterize dynamic cellular behavior. More specifically, we extract intracellular motion feature from intracellular movement field which is calculated by the optical flow techniques based on the brightness constant model (BCM) [16]. Our method is tested on 40 lymphocytes microscopic image sequences. Experimental results show that our approach is able to quantitatively illustrate the main features of a single lymphocyte's dynamic behavior and to provide new information for the diagnosis of graft rejection.

II. Methods

We segmented and tracked cell boundaries based on active contour models [17]. Those details are not presented in this paper due to space limitations. This paper focuses on the analysis of single cell dynamic behavior. When we have obtained cell boundaries, the next step is to describe the cell shape in a concise, quantitative, and biologically-relevant way. The shape features we have used in this paper are area, perimeter, eccentricity, circularity, average bending energy, rectangularity, convexity and solidity. These shape features are defined for the static object [3, 18]. Here we deduce the shape and the deformation feature descriptors for describing the morphology of the object in an image sequence as follows.

A. Cell shape features description

The accurate description of the cell shape in an image sequence is the prerequisite of cell deformation analysis. We define V_{shape} to describe the shape feature of the object in the image sequence:

$$V_{shape} = \frac{1}{N}\sum_{i=1}^{N} D_i \tag{1}$$

where N is the total number of frames in the sequence; D_i is the shape feature of the object-cell in the i-th frame (there is only one object-cell in each frame), which can be any shape feature mentioned before (area, perimeter, eccentricity, circularity, average bending energy, rectangularity, convexity or solidity). V_{shape} is regarded as the average shape feature of the cell in the image sequence, indicating the shape feature of the object in the image sequence.

B. Cell deformation features description

We define $V_{deformation}$ to describe the shape change feature of the cell in the image sequence:

$$V_{deformation} = \frac{1}{N-1}\sum_{i=2}^{N} \left| D_i - D_{i-1} \right| \tag{2}$$

where N and D_i are the same as in (1); $V_{deformation}$ is regarded as the average shape change difference of the cell in the image sequence, which indicates the deformation feature of the object in the image sequence. The $V_{deformation}$ with regards to the area and the perimeter are normalized.

C. Intracellular motion features based on optical flow

The optical flow computation is a key technique for object motion analysis, which is the distribution of the apparent velocities of brightness movement patterns in adjacent images. The optical flow constraints equation based on the BCM is shown as follows [16]:

$$I_x \cdot u + I_y \cdot v + I_t = 0 \tag{3}$$

where $I(x, y, t)$ denotes the image brightness at the point (x, y) in the image at time t. I_x, I_y and I_t are the partial derivatives of the image brightness with respect to x, y and t, respectively. (u,v) is the optical flow velocity. The details of the solution process can be found in [16].

We define V_{motion} to describe the intracellular motion feature as follows:

$$V_{motion} = \frac{1}{M}\sum_{i=1}^{M} V_{MeanVeloField}(i) \tag{4}$$

where $V_{MeanVeloField}(i)$ is the mean velocity of the intracellular motion field (which is the same as the optical flow field) at the i-th frame, and M is the total number of frames of the optical flow fields in the image sequence. The mean velocity of each intracellular motion field is computed by:

$$V_{MeanVeloField} = \frac{1}{A(\Omega)} \sum_{(x,y)\in\Omega} \sqrt{u^2(x,y) + v^2(x,y)} \tag{5}$$

where $u(x, y)$ and $v(x, y)$ are the horizontal and vertical components of the velocity at the point (x, y). $A(\Omega)$ is the area of the region Ω which is a closed two-dimensional optical flow field domain:

$$\Omega = \left\{ (x, y) : \sqrt{u^2(x, y) + v^2(x, y)} \geq threshold \right\} \tag{6}$$

Here, $threshold = 0.0001$, which is used to restrict the edge of the optical flow field.

III. EXPERIMENTS

A. Materials preparation

Two sets of experiments were conducted to obtain the cell image sequences. The first experiment was conducted through autologous transplant; healthy Balb/C male mice were used as both hosts and donors, which was the self-skin transplantation group (SST group). The second experiment was conducted through allogenic transplantation, in which healthy Balb/C male mice were used as hosts while healthy C57BL/6 male mice were used as donors. This was the allogenic skin transplantation group (AST group). The lymphocytes in the AST group showed irregular dynamic behavior and were more active when compared to the SST group.

The lymphocyte image sequence (20~30 seconds, 500~700 frames) was obtained through an optical phase contrast microscope at a magnification of 16000 from the blood samples that were collected from the tails of the mice (6-8 weeks, 20-22g) 7 days after the skin transplantation. Our data consists of 40 image sequences (20 from each of the two groups).

B. Experiments on cell shape and deformation features extraction

We selected the first 500 sequential frames from the images sequence. Then the 500 frames were sampled uniformly (selecting every tenth frame) to form a 50-frame clip. We segmented and tracked the cell boundaries in each frame from the 50-frame clip. The boundaries of the cells are shown as the solid line in Fig. 1.

The V_{shape} and $V_{deformation}$ were computed from each clip according to (1) (2), respectively. The values that are useful in differentiating between the two test groups are shown in Fig. 2 (V_{shape} of circularity, convexity and solidity; $V_{deformation}$ of area, perimeter, circularity, convexity and solidity). The horizontal axis denotes the serial number of the image sequence and the vertical axis is the value of the V_{shape} or $V_{deformation}$.

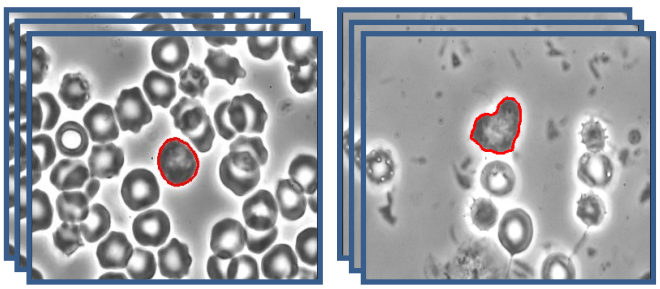

(a) from SST group (b) from AST group.

Figure 1. Image sequences observed through a phase contrast microscope.

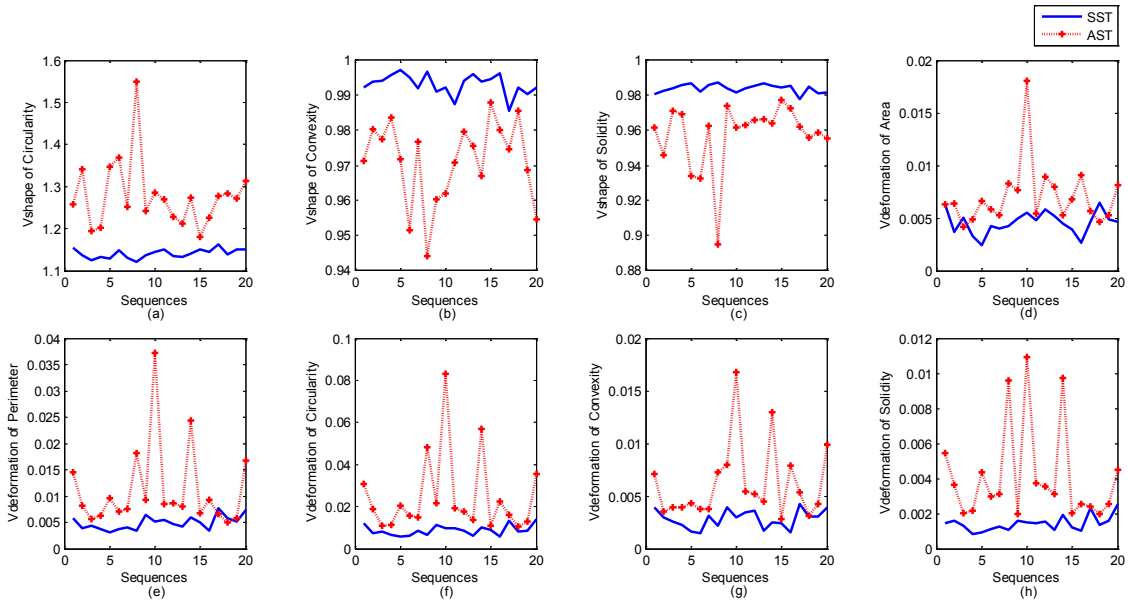

Figure 2. The shape and deformation descriptors of 40 image sequences (20 from each of the two groups).

There are distinct differences between two groups of data in regards to shape: V_{shape} of circularity, convexity and solidity (as shown in Figs. 2(a)-(c). Differences also exist in $V_{deformation}$ of deformation features, as demonstrated in Figs. 2(d)-(h). The other considered features (V_{shape} of area, perimeter, eccentricity, average bending energy, rectangularity; $V_{deformation}$ of eccentricity, average bending energy, rectangularity) are insignificant and are omitted in Fig. 2.

C. *Experiments on intracellular motion features extraction*

The intracellular motion field was computed according the optical flow techniques discussed in Section II-C. Pairs of images taken at an interval of 4 (frames 1 and 5, 2 and 6…) were used to create an optical flow field. 46 different optical flow fields were obtained from each 50-frame clip. One optical flow field is shown in Fig. 3(c), where each vector displays the sampled velocity of 5×5 pixels. The direction and the length of the arrow denote the direction and the magnitude of the velocity of intracellular motion, respectively.

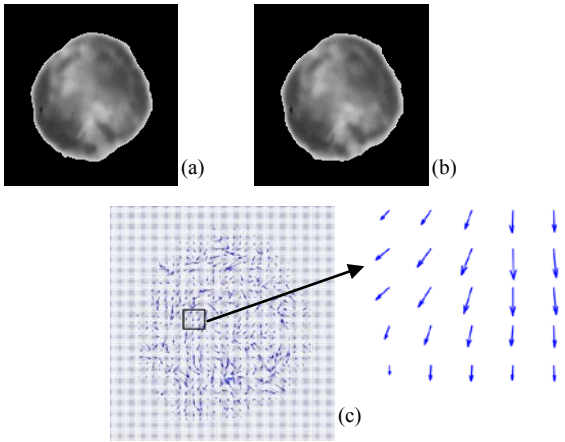

Figure 3. (a) The n-th frame image. (b) The (n+4)-th frame image. (c) The optical flow field computed from the two adjacent frames.

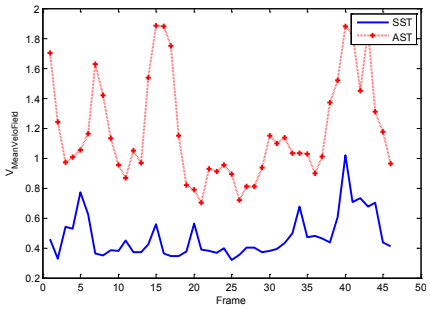

Figure 4. Evolution with frame of the mean velocity extracted from two image sequences.

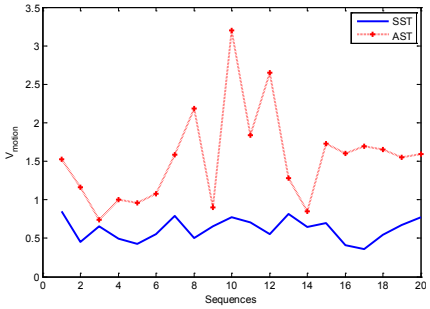

Figure 5. The intracellular motion features of 40 image sequences (20 from each of the two groups).

The evolution with frame of the $V_{MeanVeloField}$ extracted from two image sequences are shown in Fig. 4. We then extracted the motion feature from each clip according to equation 4. The results are shown in Fig. 5, which demonstrates that the speed of intracellular movement in the AST group is faster than in the SST group. This is consistent with the clinical observation in this study.

D. Cell dynamic behavior classification by the probabilistic neural network (PNN)

We extracted the shape, deformation and intracellular motion features of the cell from 40 image sequences, which are shown in Fig. 2 (shape and deformation) and Fig. 5 (intracellular motion), respectively. Then we used the shape descriptors of circularity, convexity and solidity, the deformation descriptors of area, perimeter, circularity, convexity and solidity, and the V_{motion} to form a 9-parameter feature vector (S&D&M-features) to characterize the cell dynamic behavior in an image sequence. PNN was used to classify the SST and AST categories with 10-folder cross-validation. A 9-parameter feature vector was extracted from each clip, and used as the input of PNN. In each trial, we randomly select nine tenths of data for training, and one tenth of them for testing. All the classification experiments were randomly repeated 100 times. Additionally we compared our results with several other schemes such as using shape features only (S-features: V_{shape} of the circularity, convexity and solidity); using deformation features only (D-features: $V_{deformation}$ of the area, perimeter, circularity, convexity and solidity); or using the motion feature only (M-feature: V_{motion}).

The classification rates of the two groups are shown in Table I, namely the comparison results of sensitivity (Sen: the probability that the test reports that an image sequence is from the AST group when in fact it is from the AST), specificity (Spe: the probability that the test reports that an image sequence is from the SST when in fact it is from the SST), false positive (FaP: the probability of an AST result when in fact an image sequence is from the SST group), false negative (FaN: the probability of an SST result when in fact an image sequence is from the AST group), and mean recognition (MRe: the average correct recognition rate). For our test, it typically takes about 0.3 second to run PNN with MATLAB 2012 implemented on a 2.93 GHz CPU, 4.00 G RAM personal computer.

TABLE I. CLASSIFICATION RESULTS BY PNN

Ratio / Features	Sen (%)	Spe (%)	FaP (%)	FaN (%)	MRe (%)
S	88.39	91.87	8.44	11.21	90.13
D	89.88	90.15	9.87	10.07	90.03
M	86.26	85.88	14.05	13.80	86.08
S&D&M	94.82	97.83	2.22	5.05	96.33

Table I shows that the highest recognition rates are achieved with the combined shape, deformation and intracellular motion features.

IV. CONCLUSION

We have proposed a scheme for quantitatively analyzing the shape, deformation, and intracellular motion of a lymphocyte in intravital microscopic image sequences, and have applied it to the study of the dynamic behavior of a single lymphocyte. The contribution of the proposed method can be concluded in two aspects: first, we have computed the velocity of intracellular movement field using optical flow techniques and extracted motion features from it. Second, we have presented a comprehensive quantitative analysis of the dynamic behavior of lymphocytes by combining features of cell shape, deformation, and intracellular motion. Experimental results show that the extracted features can be used to characterize the cellular dynamic behavior, leading to potential applications to the research of the single cell dynamic behavior, such as the assisted diagnosis of graft rejection.

REFERENCES

[1] R. Ananthakrishnan and A. Ehrlicher, "The forces behind cell movement," *International Journal of Biological Sciences*, vol. 3, pp. 303-317, Jun. 2007.

[2] J. R. Swedlow, "Advanced hardware and software tools for fast multidimensional imaging of living cells," *Proceedings of the National Academy of Sciences of the United States of America*, vol. 107, pp. 16005-16006, Sept. 2010.

[3] Z. Pincus and J. A. Theriot, "Comparison of quantitative methods for cell-shape analysis," *Journal of Microscopy*, vol. 227, pp. 140-156, Oct. 2007.

[4] F. Germain, A. Doisy, X. Ronot, *et al.*, "Characterization of cell deformation and migration using a parametric estimation of image motion," *IEEE Transactions on Biomedical Engineering*, vol. 46, pp. 584-600, May 1999.

[5] E. Meijering, O. Dzyubachyk, I. Smal, *et al.*, "Tracking in cell and developmental biology," *Seminars in Cell & Developmental Biology*, vol. 20, pp. 894-902, Oct. 2009.

[6] K. Solez, "History of the Banff classification of allograft pathology as it approaches its 20th year," *Current Opinion in Organ Transplantation*, vol. 15, pp. 49-51, Feb. 2010.

[7] I. Ersoy, F. Bunyak, M. Mackey, *et al.*, "Cell segmentation using Hessian-based detection and contour evolution with directional derivatives," in *Proceedings of 5th IEEE International Conference on Image Processing*, 2008, pp. 1804-1807.

[8] I. T. Young, "The classification of white blood cells," *IEEE Transactions on Biomedical Engineering*, vol. 19, pp. 291-298, Jul. 1972.

[9] G. Thurston, B. Jaggi, and B. Palcic, "Measurement of cell motility and morphology with an automated microscope system," *Cytometry*, vol. 9, pp. 411-417, Sept. 1988.

[10] F. Siegert, C. J. Weijer, A. Nomura, *et al.*, "A gradient method for the quantitative analysis of cell movement and tissue flow and its application to the analysis of multicellular dictyostelium development," *Journal of Cell Science*, vol. 107, pp. 97-104, Jan. 1994.

[11] Y. Sato, J. Chen, R. A. Zoroofi, *et al.*, "Automatic extraction and measurement of leukocyte motion in microvessels using spatiotemporal image analysis," *IEEE Transactions on Biomedical Engineering*, vol. 44, pp. 225-236, Apr. 1997.

[12] X. Ronot, A. Doisy, and P. Tracqui, "Quantitative study of dynamic behavior of cell monolayers during in vitro wound healing by optical flow analysis," *Cytometry*, vol. 41, pp. 19-30, Sept. 2000.

[13] K. Keren, Z. Pincus, G. M. Allen, *et al.*, "Mechanism of shape determination in motile cells," *Nature*, vol. 453, pp. 475-480, May 2008.

[14] M. K. Driscoll, J. T. Fourkas, and W. Losert, "Local and global measures of shape dynamics," *Physical Biology*, vol. 8, pp. 055001(1-9), Aug. 2011.

[15] X. An, Z. Liu, Y. Shi, *et al.*, "Modeling dynamic cellular morphology in images," in *Proceedings of the 15th International Conference on Medical Image Computing and Computer Assisted Intervention*, 2012, pp. 340-347.

[16] B. K. P. Horn and B. G. Schunck, "Determining optical flow," *Artificial Intelligence*, vol. 17, pp. 185-203, Aug. 1981.

[17] B. Li and S. T. Acton, "Active contour external force using vector field convolution for image segmentation," *IEEE Transactions on Image Process*, vol. 16, pp. 2096-2106, Aug. 2007.

[18] M. Yang, K. Kpalma, and J. Ronsin, "A survey of shape feature extraction techniques," in *Pattern Recogniton*, P. Yin, Ed. 2008, pp. 43-90.